DESIGN OF SQUAT STEEL TANKS WITH R/T > 5000

P. Knoedel, Th. Ummenhofer
Ingenieurbuero Dr. Knoedel, Humboldtstrasse 25a, D-76131 Karlsruhe, Germany.
info@peterknoedel.de
Institut fuer Bauwerkserhaltung und Tragwerk, Universitaet Braunschweig, Pockelsstrasse 3, D-38106 Braunschweig, Germany.
t.ummenhofer@tu-braunschweig.de

1 Introduction

Tanks for agricultural sewage are often built in vertical cylindrical shape. Typical dimensions are 32 m diameter, 6 m height in five different strakes with wall thicknesses of 6.0 mm; 5.0 mm; 4.0 mm; 3.0 mm; 3.0 mm (from bottom to top). The strakes are joined by overlapping 50 mm and bolting, and at each overlap a cold formed C 50x100x2 section is added, so that one of the 50 mm flanges is connected to the tank, and the 100 mm wide web and the second flange are outside of the tank. Twin profiles with same dimensions are mounted at the top edge of the tank, inside and outside of the tank wall. When serving as a sewage tank, the structure might have a central mast and a cone shaped 15º textile roof, which is supported by elastic prestressed strips, spanned between the mast's top and the tank's upper edge.

The top strakes of the tank wall are having a ratio of R/T = 5300. This range of R/T is not covered by the known shell buckling design codes, which are – due to lack of experience - restricted to R/T = 2500. The absence of valid design rules made it necessary to study the structural behavior by FE method with the aim, to match the known features of ring stiffened tanks to this range of geometrical proportions.

When loaded by natural wind there are two collapse modes to be taken into consideration for the open tank without a stiff roof.

Unstiffened tank wall – global failure
: Due to the pressure onto the luff-region of the tank wall and the suction onto the lateral parts of the tank the luff-side wall of the tank will incline to the inside of the tank. There is only little stiffness to prevent this deformation, it is an strainless mode.

Stiffened tank wall – local failure
: If the tank has an eaves beam of sufficient stiffness (and/or intermediate ring-stiffeners), the luff-side tank wall will buckle locally. There should be a considerable postbuckling strength after buckling.

Ring stiffeners – global failure
: The ring stiffeners are expected to fail in multi-wave buckling along the luff-side compressive zone, or by luff-sided snapping through, which would be enhanced by the wind suction along the flanks.

There might be additional compressive forces in the top ring stiffener due to the prestressed roof-supporting strips, but this will be discussed elsewhere. This present paper is a working report on our studies towards the understandig of ring stiffened membrane shells.

2 Unresolved Questions

Recent works from Schmidt and co-workers ([BIN96], [SMI98]) were devoted to that questions. Cylinders under external pressure were investigated numerically and experimentally including postbuckling behavior. A design recommendation was given for the eaves beam. However, there are some questions which still need a closer look:

Wind pressure distribution
: The suggested pressure distribution for Reynolds' numbers of $10^7 – 10^8$ could be much to conservative. For a cylinder having an aspect ratio of more than 5 it can be taken, that most of the flow goes over the top of the cylinder, whereas only the part of the flow, which goes around the cylinder, will produce the suction at the lateral parts of the shell wall. This is formulated in a draft of prEN 1993-4-1, but will not be discussed in this paper.

Analysis of the unstiffened tank

Very often, an eigenmode analysis is performed on the unstiffened tank. As assumed above, the governing global mode is a strainless inclination of the luff-side wall. Therefore a geometrical non-linear big deformation analysis could give more realistic results.

Minimum stiffness of the eaves beam

Which stiffness of the eaves beam borders the global strainless mode from local buckling. According to Schmidt (SMI98) this minimum stiffness is not sufficient for practical design, since, along with big postbuckling deformations, the structure still might switch from a stable local buckling mode into an unstable global collapse mode.

Strength criterion for the eaves beam

According to some experience with ring stiffened shells with large cutouts, a stiffness criterion may be not sufficient to design a ring stiffener.

3 Basic Geometry

To study the above described effects the geometry of the tank was simplified to an 'academic geometry' with fixed geometry features which were used throughout the FEM runs. The shell was given a diameter of 10 m and an unstepped wall thickness of 1 mm. A height of the shell of 2 m was used in most of the cases, sometimes the results were cross-checked to a height of 5 m or 10 m. Half of the cylinder was modelled using symmetry conditions along the luff-lee symmetry axis. The bottom nodes were fixed to displacements but free to rotate, the top nodes were free. Different widths of top rings stiffeners were used, e.g. 10 mm or 100 mm. The wall thickness of the ring was chosen to be 10% of the width, in order to exclude local buckling of the ring.

4 Numerical Studies

For the finite element analyses an available numerical tool was used (ANSYS 5.3; SHELL181; wavefront solver, subspace iteration with Sturm sequence check to determine the lowest eigenvalues).

Unlike used practice in academic research, where the uncertainties of shell buckling investigations are reduced to percent, proceeding was motivated by designers point of view. Element mesh and number of substeps were chosen as coarse as possible to keep computation times short, the option of bisection was omitted in most cases. This gives only little accuracy as far as single numbers are concerned, like the 'last convergence load' might be more than 15% off the 'real' limit load of the structure, and due to the drifting off of the coarsely stepped load deflection path the bifurcation loads might be 10% too high. On the other hand this allowed to trace most of the relevant features of the problem within the time available.

A lengthy background documentation – including model description, applied loads, used substitute imperfections, load-deflection-curves, deformed shapes under load, eigenmodes – for some 80 FEM runs can be downloaded from http://www.peterknoedel.de/search/search.htm.

5 Wind Load

Wind load is assumed according to German standard DIN 1055 part 4. This might not be close to 'real' but it is a unique loading over all structural variations under investigation. As mentioned before natural wind might not develop the DIN pressure distribution when the tank is very squat, especially concerning the flank suction, since most of the flow goes over the tank and not around the sides. On the other hand – without a roof – the luff wall and the lee wall of the tank might be exposed like a single wall each, so that for both parts pressure coefficients of

$$p,\text{eff} = p,\text{luff} + p,\text{lee} = 1.0 + 0.6 = 1.6 \quad (1)$$

would have to be considered. Greiner suggested earlier [GRE95], that the luff pressure coefficient should be not more than 0.8 due to boundary layer effects ahead of the tank. For further remarks on the modeling of wind pressure distribution see Ummenhofer/Knoedel [UMM00]. For reasons of comparability with closed shells lee-suction inside the tank is not considered in the present paper.

6 Imperfections

Some time ago Knoedel and Ummenhofer suggested different patterns of initial radial shape imperfections for cylindrical shells under axial load ([KNO95], [KNO96], [UMM96]). In a recent paper Schneider proposed 'consistent geometrical substitute imperfections' to match numerical results to the empirical experience of the shell stability codes [SNE04]. Hornung found in natural size experiments, that the geometrical tolerances in DIN 18800-4 are too restrictive [HOR00]. For the present study, substitute pressure loads seemed to be more convenient instead of geometrical radial initial imperfections. In order to trigger snap-through failure of the luff-wall of the tank an additional cosine shaped patch load was imposed, which extends along a certain circumferential length of both sides of the luff meridian (e.g. 2x15º; 2x7.5º; 2x3.0º). The peak substitute pressure is normalised to the wind stagnation pressure. Other kinds of imperfections were tried for the top ring, these will be described later on.

7 Definition of Failure

Plastic effects were excluded due to the R/T-ratio of 5000.

Snap through of the structure, especially when the cylinder is unstiffened or insufficiently stiffened is identified with non-convergence of the Newton-Raphson-iteration. The last converged load level is taken as limit load. Opposite to a statement in [GOD02] the windward top shell nodes show clear nonlinear behavior for the short cylinders as well, at least within the last 10% of the maximum load. This might be due to the pinned lower edge of the cylinder in the present study instead of clamped conditions in [GOD02].

Buckling of the shell is identified with bifurcation of the equilibrium. The lowest eigenvalue is taken as critical load. The mode shapes of the lower modes are multiple-element-modes, so that they can be verified as sensible numerical results. Clustering of the modes as known from axially loaded shells was not present in most cases, the shape differences of adjacent modes were clearly to be distinguished.

Buckling of the ring could not be identified uniquely. In all cases the lowest critical loads were associated with eigenmodes, were the shell was deformed, and no technical relevant displacements could be seen with the ring. With higher modes the ring showed deformations, which were connected to the deformations of the shell, but the displacements of the ring were only as much as 20% or 30% of the displacements of the shell. A clear buckling of the ring should show the biggest displacements of the eigenmode with the ring and minor displacements with the shell. Taking the second or third lowest eigenmode as critical mode for the ring is therefor very conservative.

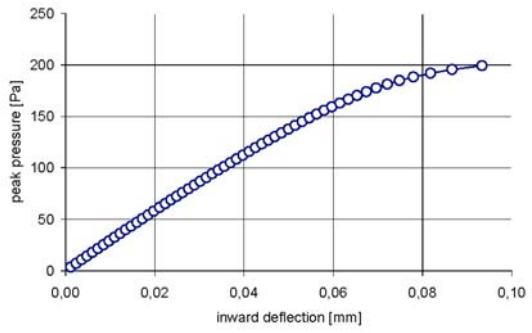

Figure 1: Load deflection curves for the unstiffened shell, p,max = 2.1*181 Pa (R/T = 5000; L/R = 0.4)

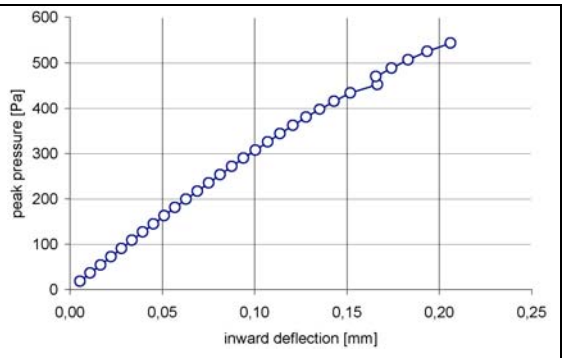

Figure 2: like fig. 1 but with top ring stiffener 100x10 mm, p,max = 3.0*181 Pa

8 Structural Behavior

8.1 Global Bending

When we started the investigation we expected, that due to the global action of the wind (pressure at the luff wall and suction at the flanks) the shell would show not very much stiffness against this loading and

the governing failure mode would be snap through of the luff wall. This mechanism was supposed to be a cos 2φ strainless membrane mode. As well the top ring should fail in a cos 2φ mode.

The structural behavior we found was somewhat different. The radial shell deformations under wind load are very small and the structure remains so stiff, that the luff wall would rather develop several vertical folds than fall in globally as known from failure of real tanks (e.g. fotograph on the backside cover of the Prague conference proceedings [KRU03]). We assume, that the global-falling-in mode is associated to a position far along the unstable postbuckling path. The postbuckling path has been studied by Godoy and Flores [GOD02], but unfortunately the deformed shapes given are close to maximum load, and do not indicate the failure mode at the (numerical) end of the postcritical path.

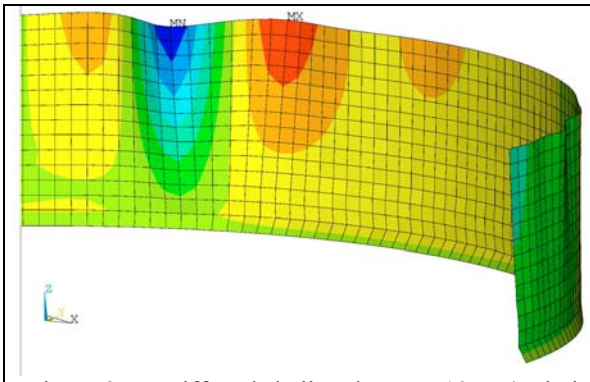

Figure 3: Unstiffened shell under DIN 1055-4 wind pressure distribution, p,max = 2.0*181 Pa, max radial deformation +0.30 mm/-0.47 mm (flank); -0.18 (luff) (R/T = 5000, L/R = 0.4)

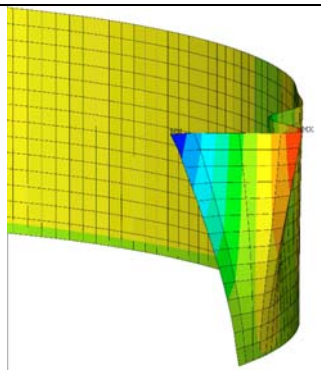

Figure 4: like fig. 3 but additional cos-shaped patch load along 2*7.5º, p,max = 2*0.60*181 Pa, max radial deformation +3.3 mm/-6.7mm

Even with the imperfections mentioned above the shell would develop single vertical folds rather than snap through. In one case, with a width of the cosine shaped pressure patch of 2x15º the luff top node went backwards against the imperfection pressure and formed an outward (!) fold, seemingly both inward folds at it's side were more effective.

8.2 Imperfection Sensitivity

As known for cylindrical shells under external pressure, the sensibility to imperfections is only moderate. The graphs for imperfection sensitivity below show, that even with gross imperfection pressures the bearing capacity of the shell does not fall under a certain limit. This might be associated with the postbuckling minimum of the structure. It is interesting to see, that even for the very sensitive cylinders under axial load there is a distinct lower bound of the bearing capacity for deep imperfections [KNO91a], [KNO91b].

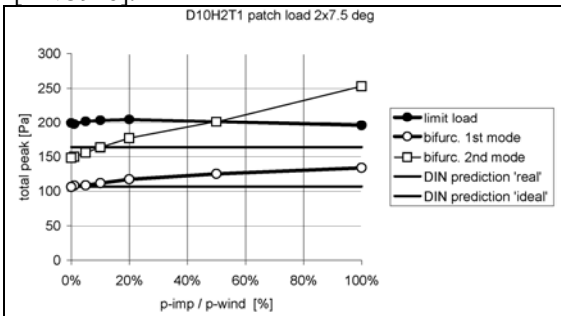

Figure 5: Imperfection sensitivity for unstiffened shell (R/T=5000; L/R=0.4)

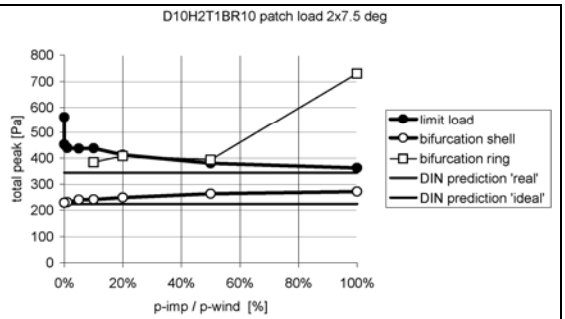

Figure 6: Imperfection sensitivity for ring stiffened shell (R/T=5000; L/R=0.4; end ring 10x1mm)

8.3 End Ring Stiffener

As an example an outside top ring with the dimensions of only 10 mm width and 1 mm wall thickness was investigated. Of course this is insufficient stiffening since there is a common failure mode for shell and ring, but even this small ring increased snap-through-pressure of the shell by at least 50%.

According to Binder [BIN96] – based on Ansourian [ANS92] and Blackler [BLA88] – the ring should have a stiffness, and – based on [DASt017] – a strength of

$$I,cr = 0.048 * T^3 * H$$
$$W = 7*10^{-8} * D^2 * H * p,d / 3\ kN/m^2 \quad (2)$$

where p,d = 3 kN/m^2 is a conservative estimate for the design wind stagnation pressure at the luff wall, including uniform suction on the inside surface of the cylinder. For the shell presented below with L/R = 2 and with p,d = 1.5 * 0.8 kN/m^2 = 1200 Pa this properties would amount to

$$I = 0.048 * 1^3\ mm^3 * 10000\ mm = 480\ mm^4$$
$$W = 7*10^{-8} * 10000^2\ mm^2 * 10000\ mm * 1200\ Pa / 3000\ Pa = 28\ cm^3 \quad (3)$$

for the shell with L/R = 0.4 it would be

$$I = 480\ mm^4 / 5 = 96\ mm^4$$
$$W = 28\ cm^3 / 5 = 5.6\ cm^3 \quad (4)$$

The small ring stiffener above has properties of (without additional effective width of the shell)

$$I = 10^3\ mm^2 * 1\ mm / 12 = 83\ mm^4$$
$$W = 10^2\ mm^2 * 1\ mm / 6 = 17\ mm^3 \quad (5)$$

The heavy stiffener has properties of

$$I = 100^3\ mm^2 * 10\ mm / 12 = 83\ cm^4$$
$$W = 100^2\ mm^2 * 10\ mm / 6 = 17\ cm^3 \quad (6)$$

Note, that the criterion for Ansourian and Blackler were zero deflections of the ring in the eigenmode of the structure. This criterion was not coupled to any strength gains in the shell.

In order to trigger failure in the heavy ring we used 3 different techniques. First attempt was the above described patch load around the luff meridian. We reduced the circumferential width of the patch load to 3.0º in order to enforce local failure of the ring.

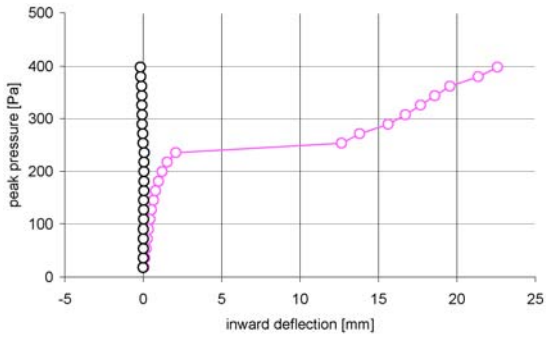

Figure 7: load-deflection behavior of characteristic luff nodes: top (black) and mid-height (pink); (R/T=5000; L/R=0.4, end ring 100x10mm)

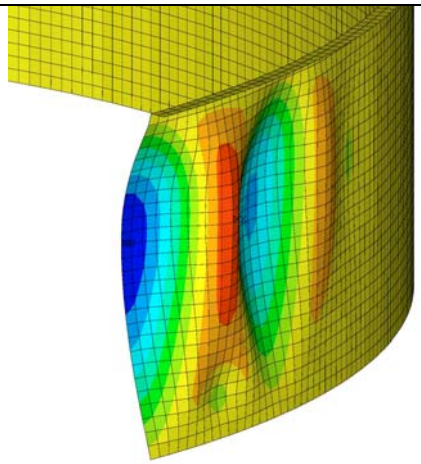

Figure 8: see fig. 7: deformed shape at last convergence for DIN-wind + patch load p,max = (1 + 0.5)*2.20*181Pa = 600 pa

Note, that the red marked area at the deformed shape in fig. 8 indicates an outward deflection of 5 to 9 mm, i.e. against the wind. The maximum inward deflection of the luff meridian is 23 mm. The number of circumferential waves in 'classical buckling' according to Greiner's approximation is 41 for constant external pressure. A linear eigenvalue analysis under constant external pressure gave 60 full waves. This might be due to the fact, that the 'pinned-end' boundaries of a FE calculation are giving more axial stiffness to the shell's ends, as is assumed in the classical equations. This makes the FE-shell having a smaller effective meridional length, which in turn accounts for the higher wave number. The two outward bulges of the above shell have a distance of about 12º, which corresponds to 30 circumferential full waves. This could indicate that there is too much bending stiffness in the FE-shell, and it should have been modeled with half the element size to get effects properly. On the other hand this should be only a secondary effect in our attempt to trigger failure in the ring.

The top luff node moves inward up to p = (1 + 0.5)*1.30*181 Pa = 350 Pa (shoulder of the load-displacement line), and then reverses to an outward deflection where it ends at +0.2 mm. It seems, that both inward bulges of the shell produce a stiff rib in between, so this does not seem to be a way to bring the ring to failure numerically.

Second technique was to apply separate radial loads to the ring, so the ring should buckle in a multi-wave mode. If the radial line load was applied in a shape, which corresponds to the failure mode of the ring, the ring should exhibit snap-through failure. In a check with a constant radial load and linear buckling analysis the lowest eigenvalue was a load of 63 N/mm with 10 circumferential waves. Up to the seventh eigenvalue at 85 N/mm there were mode shapes between 8 and 14 full waves. Regarding the fact, that present design codes suggest a critical mode of 2 waves for the ring, we choose the lowest of those modes for the shape of the radial edge load, which was then represented by

$$p,e = p,e,hat * \cos(8*\varphi) \quad . \tag{7}$$

We intended to calibrate the peak value p,e,hat thus, that the ring would have deflections of ±6.5 mm, which would be L/300 for each half wave of the ring - a common measure for substitute imperfections with steel structures. Last convergence was at p,e,hat = 4 N/mm, far below the linear critical load, with a maximum radial deflection of the ring of ±2.5 mm. At that state there were meridional membrane compressive stresses below the outward waves of the ring, which had reached the critical level for axial buckling, roughly 25 N/mm^2 for that shell geometry. Subsequently elephant's feet formed at that portions of the shell, along with vertically inclined stiffening folds from top to bottom (see fig. 9). The same effect could be observed with a cylinder of 10 m height (see fig. 10). At a radial load of p,e,hat = 11.4 N/mm and maximum inward deflection of the luff top node of 55 mm there were compressive stresses at the bottom of up to 38 N/mm^2 in very localised areas, which marked end of convergence.

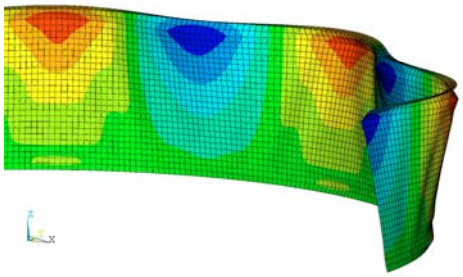

Figure 9: deformed shape for a cosine shaped line load along the top edge;
(R/T=5000; L/R=0.4, end ring 100x10mm)

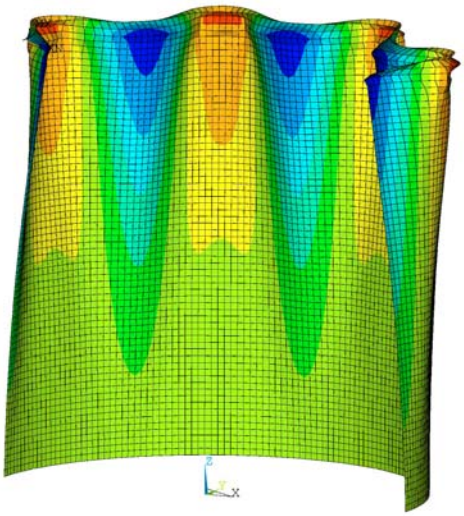

Figure 10: deformed shape for a cosine shaped line load along the top edge;
(R/T=5000; L/R=2.0, end ring 100x10mm)

Again, for the squat and the high cylinder as well, this seemed to be no successful way to trigger snap-through failure in the ring.

Third technique was 'classical' use of geometrical radial shape deviations, derived from linear eigenvalue analysis. We put the squat shell under constant external pressure and performed a linear eigenvalue analysis. The shape of the lowest eigenmode, which is associated to a critical stagnation pressure of 765 Pa and which has 60 circumferential waves, was taken to generate the geometrical initial radial deformations of the structure with a maximum amplitude of 10 mm, i.e. w0/T = 10. Then a geometrical non linear large deflection analysis was performed for constant external pressure as well. Last convergence was found at p,max = 3000 Pa. In that state, the shell had additional radial displacements of 34 mm (and 22 mm alternatively) to the inside, so that vertical ribs were formed with a depth of 12 mm like a corrugated sheet. There were no considerable compressive circumferential stresses in the shell wall, but the vertical ribs were loaded in bending action. Again, no failure of the ring could be produced.

8.4 Multi Ring Stiffening

The multi ring stiffened tank was simplified as well, in order to reduce the number of geometrical parameters. The dimensions are: D = 30 m; H = 6 m; T = 2.0 mm unstepped. The overlap between the strakes and the inner flange of the ring stiffeners was not modeled, so the rings are sections L100x50. Five rings were placed at a vertical distance of 1200 mm, the top ring section was modeled only outside, the twin section at the inside was omitted. This geometry gives a conservative estimate of the real tank's

structural behavior, because there is more cross-section in the lower strakes, in the overlap joints and rings, and the top ring is doubly stiff.

Due to the restrictions of space given for this paper the results can not be shown in detail. It can be noted however, that the multi-ring-stiffened structure exhibits an even more benign behavior as described above. On first hand this is due to the fact, that the shell segments have a ratio L/R = 0.080 (and R/T = 7500). The design value for constant external pressure is 358 Pa according to DIN, which means, that with a closed textile roof the shell would not even buckle under most middle-european wind conditions. The rings are stiff enough to transfer the luff-side pressure loads to the flanks without being stressed very much in bending.

9 Conclusions

- When looking for the stability of a shell under external pressure (as well as under axial load) it is definitely not sufficient to impose geometrical or load imperfections and perform a large deflection limit load analysis, as is recommended e.g. in the ANSYS manual. Bifurcation beyond the limit load is likely, which must be checked in a separate bifurcation analysis (which has been stated in [HOR00] as well). In a recent paper Schneider is pointing out, that there is no such thing as 'the most unfavourable imperfection' [SNE04a]. According to Schneider the most unfavourable imperfection pattern depends on the imperfection amplitude and can not be uniquely determined [SNE04b].

- The snap through of an unstiffened cantilever shell does not seem to be a strainless mode, if the bottom edge is anchored properly. Even very flat and very thin shells can supply arching action, if the pressure patches are not smaller than 2x10º.

- The buckling of an edge-supported shell or shell panel under wind load, i.e. uneven circumferential pressure, can be very well described according to a local-maximum-stress concept, where 'local' means 10° in circumferential direction. The capability of ring stiffened shells or shell sections to develop postcritical strength is well known.

- The imperfection sensitivity against snap through has a distinctive lower bound even for intense additional patch loads.

- The design of end rings according to a cos(2*φ)-failure-hypothesis is very conservative. If the ring deflects in a cos(n*φ)-manner with finite deformations, even a membrane shell can support the ring by activating shear and meridional stresses. As is known from postcritical web-behaviour with welded I-sections, transfer of shear forces is not very much reduced, when the shell itself is in a postcritical state. Of course, the capability of transferring radial forces via shear and meridional membrane action to the foundation would be reduced, if there is the possibility of uplift at the lower shell edge. May be, parts of millimeters due to the elastic deformation of a T-shaped tank foot with eccentric anchoring are enough, to change the above described behavior.

- Real tanks built as described above with intermediate ring stiffeners seem to have very benign structural behavior, as far as postcritical deformations of the shell sections can be accepted with respect to serviceability.

10 Acknowledgements

Hard- and software for the presented FEM calculations have been sponsored by ANAKON, Karlsruhe. Their support is gratefully acknowledged.

11 References

[DIN1055-4] German code DIN 1055 part 4 (1986): "Design loads for buildings; live loads, wind loads on structures not susceptible to vibrations".

[DASt017] DASt Richtlinie 017: Beulsicherheitsnachweise für Schalen – spezielle Fälle – . Entwurf 1992. Deutscher Ausschuß für Stahlbau, Stahlbau-Verlagsgesellschaft.

[ANS92] P. Ansourian (1992), "On the buckling analysis and design of silos and tanks", Journal Constructional Steel Research 23 (1992), pp. 273-294 (cited after [BIN96]).

[BIN96] B. Binder (1996), "Stabilität einseitig offener, verankerter, aussendruckbelasteter Kreiszylinderschalen unter besonderer Berücksichtigung des Nachbeulverhaltens", Diss. Universität Essen.

[BLA88] M.J. Blackler (1988), "Buckling of Steel Silos under Wind Action", Silos – Forschung und Praxis, Tagung '88 in Karlsruhe, pp. 319-330 (cited after [BIN96]).

[GRE98] R. Greiner (1998), "Cylindrical shells: wind loading", chapter 17 in C.J. Brown, J. Nielsen (eds), "Silos – Fundamentals of theory, behaviour and design", E&FN Spon, London 1998.

[GOD02] L.A. Godoy, F.G. Flores (2002), "Imperfection sensitivity to elastic buckling of wind loaded open cylindrical tanks.", Structural Engineering and Mechanics Vol. 13, No. 5 (2002) – downloaded from the internet.

[HOR00] U. Hornung (2000), "Beulen von Tankbauwerken unter Außendruck", Diss. Universität Karlsruhe.

[KNO91a] P. Knödel, A. Thiel (1991), "Zur Stabilität von Zylinderschalen mit konischen Radienübergängen unter Axiallast", Stahlbau 60 (1991), pp. 139-146.

[KNO91b] P. Knoedel (1991), "Cylinder-Cone-Cylinder Intersections under Axial Compression", pp 296-303 in: J.F Jullien (ed.), "Buckling of Shell Structures, on Land, in the Sea and in the Air", Elsevier Applied Science, London 1991.

[KNO95] P. Knoedel, Th. Ummenhofer, U. Schulz (1995), "On the Modelling of Different Types of Imperfections in Silo Shells", EUROMECH Colloquium 317, University of Liverpool, 21.-23. March 1994. Thin-Walled Structures 23 (1995), pp. 283-293.

[KNO96] P. Knoedel, Th. Ummenhofer (1996), "Substitute Imperfections for the Prediction of Buckling Loads in Shell Design", Proc., Imperfections in Metal Silos – Measurement, Characterisation and Strength Analysis, pp. 87-101. BRITE/EURAM CA-Silo Working Group 3: Metal Silo Structures. International Workshop, INSA, Lyon, 19.04.96.

[KRU03] V. Krupka (ed). (2003), Proc., Int. Conf. "Design, Inspection, Maintenance and Operation of Cylindrical Steel Tanks and Pipelines", Prague, Czech Republic, 8.-11. Oct. 2003.

[SMI98] H. Schmidt, B. Binder, H. Lange (1998), "Postbuckling strength design of open thin-walled cylindrical tanks under wind load", Thin-Walled Structures (1998) 203-220.

[SNE04a] W. Schneider (2004), "Konsistente geometrische Ersatzimperfektionen für den numerisch gestützten Beulsicherheitsnachweis axial gedrückter Schalen", Stahlbau 73 (2004), Heft 4.

[SNE04b] W. Schneider (2004), "Die "ungünstigste" Imperfektionsform bei stählernen Schalentragwerken – eine Fiktion?", submitted to Bauingenieur 79 (2004) - cited after [SNE04a].

[UMM96] Th. Ummenhofer, P. Knoedel (1996), "Typical Imperfections of Steel Silo Shells in Civil Engineering", Proc., Imperfections in Metal Silos – Measurement, Characterisation and Strength Analysis, pp. 103-118. BRITE/EURAM concerted action CA-Silo Working Group 3: Metal Silo Structures. International Workshop, INSA, Lyon, 19.04.96.

[UMM00] Th. Ummenhofer, P. Knoedel (2000), "Modelling of Boundary Conditions for Cylindrical Steel Structures in Natural Wind", Paper No. 57 in M. Papadrakakis, A. Samartin, E. Onate (eds.): Proc., Fourth Int. Coll. on Computational Methods for Shell and Spatial Structures IASS-IACM, June 4-7, 2000, Chania-Crete, Greece.